European Journal of Clinical Pharmacy
Print ISSN: 2385-409X **Online ISSN**: 3105-0409
Website: https://farmclin.com/

Original Research Article

Design, Optimization, and In Vitro–In Vivo Evaluation of Febuxostat-Loaded Nanostructured Lipid Carriers for Gout management

Article History:

Received: 11-11-2025
Revised: 26-11-2025
Accepted: 09-12-2025
Published: 24-12-2025

Name of Author:
*[1]ASHISH SHANKER MISHRA, [2]SHIKHA SHARMA

Affiliation: *[1,2]Department of Pharmaceutical Sciences, Lords University, Alwar, Rajasthan*

Corresponding Author:
Ashish Shanker Mishra

Abstract: Gout is a metabolic disorder which causes inflammation of the joints. The pain can be relieved by taking anti-inflammatory or pain-relieving medication. Febuxostat, a xanthine oxidase inhibitor is also used in the treatment of gout. It is a weak acid (pKa 3.08) and is therefore, practically insoluble in water. Due to its limited solubility in water and susceptibility to enzymatic degradation in intestine and liver, its oral bioavailability is affected. The presence of food also decreases its maximum plasma concentration (Cmax) by 39%. Hence, transdermal route is preferred for its administration. In the present research, NLCs were selected for Febuxostat delivery because of their penetration enhancing ability. NLCs containing Febuxostat were prepared using thin film hydration method. A Box–Behnken experimental design with three factors at three levels was used to investigate how the ratio of solid to liquid lipids (X_1), stirring speed (X_2), and emulsifier level (X_3) influenced the encapsulation efficiency (Y_1), drug release rate (Y_2), and overall yield (Y_3). Parameters contribution was determined using a 3-D response curve. an entrapment efficiency of 72.98%, a drug flux of 136.19 µg/cm²/h, and a yield of 92.89%. The particles were approximately 344 nm in size, with a PDI of 0.309 and a zeta potential of −22.67 mV, indicating good stability. These NLCs provided a controlled drug release in laboratory tests, demonstrating their promise as a delivery system for Febuxostat in gout treatment. Developed NLC were also in vivo evaluated in rats using local inflammation by monosodium urate crystal. The developed NLCs optimized formulation found to relieve the inflammation. Finally it was concluded that this focused research has developed a potential formulation for management of gouty arthritis.

Keywords: Gout, NLC, Febuxostat, Bioavailability, Box-Behnken design, optimization.

INTRODUCTION

Gout is a chronic metabolic and inflammatory disorder characterized by the deposition of monosodium urate (MSU) crystals in joints and periarticular tissues as a consequence of sustained hyperuricemia. Under physiological conditions, uric acid remains soluble up to a concentration of approximately 6.7–7.0 mg/dL; levels beyond this threshold promote nucleation and crystallization of urate in synovial fluid and connective tissues [1,2]. The accumulation and persistence of MSU crystals trigger intense inflammatory responses involving leukocyte infiltration, release of pro-inflammatory mediators, and recurrent episodes of acute arthritis, ultimately leading to chronic joint damage if left untreated [3,4]. Uric acid is the terminal product of purine metabolism in humans, generated through the sequential oxidation of hypoxanthine to xanthine and xanthine to uric acid, both reactions being catalyzed by the enzyme xanthine oxidase (XO). Pharmacological management of gout primarily focuses on reducing serum uric acid levels either by inhibiting uric acid synthesis using XO inhibitors or by enhancing renal uric acid excretion through uricosuric agents [5]. Commonly prescribed medications include non-steroidal anti-inflammatory drugs (NSAIDs), colchicine, corticosteroids, allopurinol, probenecid, and febuxostat [6]. Febuxostat is a non-purine selective xanthine oxidase inhibitor that has demonstrated superior urate-lowering efficacy compared to allopurinol, particularly in patients with allopurinol intolerance

or resistance [7]. Despite its therapeutic advantages, the clinical utility of febuxostat is compromised by its poor aqueous solubility, weakly acidic nature (pKa ≈ 3.08), and susceptibility to enzymatic degradation in the intestine and liver, resulting in variable and limited oral bioavailability. Additionally, food intake significantly reduces its maximum plasma concentration, further contributing to inconsistent therapeutic outcomes [8,9]. These limitations highlight the need for an alternative delivery approach capable of bypassing first-pass metabolism and improving drug bioavailability. Transdermal drug delivery offers several advantages over conventional oral administration, including avoidance of gastrointestinal degradation and hepatic first-pass metabolism, sustained plasma drug levels, reduced dosing frequency, and improved patient compliance. However, effective transdermal delivery of lipophilic drugs such as febuxostat requires suitable carrier systems capable of enhancing skin permeation while maintaining drug stability [10]. Nanostructured lipid carriers (NLCs) have emerged as a promising second-generation lipid nanoparticle system designed to overcome the limitations of solid lipid nanoparticles (SLNs). NLCs consist of a carefully optimized mixture of solid and liquid lipids stabilized by surfactants, resulting in an imperfect lipid matrix that provides higher drug-loading capacity, improved stability, and controlled drug release characteristics [11–13]. Owing to their nanoscale size, lipid composition, and occlusive properties, NLCs enhance skin hydration and penetration, making them particularly suitable for transdermal drug delivery of poorly water-soluble drugs [14]. To achieve an optimized formulation with desirable physicochemical and performance attributes, a systematic statistical approach is essential. Design of Experiments (DoE), particularly the Box–Behnken design, is a robust and efficient optimization technique that evaluates the individual and interactive effects of multiple formulation and process variables with a reduced number of experimental runs. This approach enables the development of predictive models for critical quality attributes such as encapsulation efficiency, drug release, and yield, ensuring reproducibility and formulation robustness [15–17]. In this context, the present study aims to develop and optimize febuxostat-loaded nanostructured lipid carriers using a Box–Behnken experimental design. The influence of solid-to-liquid lipid ratio, stirring speed, and emulsifier concentration on encapsulation efficiency, drug flux, and percentage yield was systematically investigated. Furthermore, the optimized NLC formulation was characterized for particle size, zeta potential, morphology, and in-vitro drug release behavior. The therapeutic potential of the developed NLC gel was further evaluated through in-vivo anti-inflammatory studies using a monosodium urate crystal-induced gout model in rats. Overall, this research seeks to establish a promising transdermal nanocarrier system for improving the bioavailability and therapeutic efficacy of febuxostat in the management of gouty arthritis

MATERIALS & METHODS

All ingredients used were of analytical grade. Febuxostat was procured from Yuventis Pharmaceuticals Baddi, HP, India. All solvents were purchased from Qaulikems. Compritol 888 ATO and Capryol 90 were obtained from Gattefosse India. Tween 80 and Poloxamer 188 were purchased from Sigma-Aldrich (Mumbai, India).

Preparation of NLC

Preparation of Lipid phase: weigh and melt the solid lipid compritol and mix with liquid lipid capryol 90 at above the 5-10 degree above the melting point of the solid lipid. Dissolve the drug Febuxostat in the melted liquid. Preparation of Aqueous phase was done by a hot aqueous phase solution of surfactant tween 80/ poloxamer 188 at the same temperature as the lipid phase.and add necessary co surfactant. Emulsification was done under high speed magnetic stirrer add aqueous phase to lipid melt dropwise to form O/W emulsion. Use high shear homogenizer for 5-10 mins pulse mode to form nanoEmulsion. Solidification by cooling was done by submerging the Nanoemulsion into cold water/ice container for 2 hours to induce solidification of liquid globules as NLCs [18-19]. The experimental design of all 17 batches of NLCs is shown in table 1.

Table 1: Independent Variables and their Levels in BBD

Formulation Variables	Low (−1)	Medium (0)	High (+1)
X1: Solid lipid to Liquid lipid ratio	75:25	80:20	85:15
X2: Stirring Speed (rpm)	1500	2000	2500
X3: Emulsifier Concentration (% v/v)	1.5	2.0	2.5

Formulation optimization

Box-Behnken Design

To study the effect of three independent variable X1 (Solid lipid to liquid lipid ratio), X_2 Stirring speed (rpm), X_3 Emulsifier concentration (% v/v). on the following dependent responses Y_1: Entrapment Efficiency (% w/w), Y_2: Drug Flux (µg/cm²/h),Y_3: Percentage Yield (% w/w), Each factors were assessed at 03 di]fferent levels (−1, 0, +1). A total of 17 experimental runs were generated, including 12 factorial points and 5 center points to evaluate experimental error and model adequacy as shown in table 2.

Table 2: Experimental Runs for Box-Behnken Design

Batch No.	X1: Lipid Ratio	X2: Stirring Speed (rpm)	X3: Emulsifier Conc. (% v/v)
B1	-1	-1	0
B2	1	-1	0
B3	-1	1	0
B4	1	1	0
B5	-1	0	-1
B6	1	0	-1
B7	-1	0	1
B8	1	0	1
B9	0	-1	-1
B10	0	1	-1
B11	0	-1	1
B12	0	1	1
B13	0	0	0
B14	0	0	0
B15	0	0	0
B16	0	0	0
B17	0	0	0

Characterization of NLCs

Determination of Entrapment Efficiency

To determine the entrapment efficiency, an accurately weighed quantity (50 mg) of the NLC formulation was dispersed in phosphate buffer (pH 6.8) and subjected to extraction for 24 hours. After equilibration, the dispersion was centrifuged at 3500 rpm for 10 minutes, and the supernatant was collected. The concentration of free (unentrapped) Febuxostat was quantified using a UV-Visible spectrophotometer at λ 317 nm. The percent entrapment efficiency was calculated using the following equation:

Entrapment Efficiency (%) = {Total Drug} - {Unentrapped Drug} X 100
{Total Drug}}

Determination of Drug Flux

In vitro permeation studies were carried out using a Franz diffusion cell, where a pre-treated dialysis membrane (MWCO 12,000–14,000 Da) was mounted between the donor and receptor compartments. The effective surface area of the membrane was 2.54 cm², and the receptor compartment contained 20 mL of phosphate buffer (pH 6.8) maintained at 37 ± 0.5°C under constant stirring at 200 rpm.

Febuxostat-loaded NLCs were applied to the donor compartment, and aliquots (0.5 mL) were withdrawn at predetermined intervals up to 24 hours. Each sample was replaced with fresh buffer. The amount of drug permeated was measured spectrophotometrically, and the flux (J) was calculated from the slope of the linear portion of the cumulative drug release vs. time plot

$$J = Q/(A \times t)$$

Where, Q is Quantity of drug that transverse membrane in time t. A is Area of diffusion (cm^2)

J is Flux ($\mu g/cm^2h^{-1}$)

Determination of Percentage Yield

The percentage process yield was calculated by accurately weighing the total dried NLCs obtained after lyophilization or vacuum drying. The formula used was:

Yield (%) = {Weight of Dried NLCs}}{Total Weight of Lipids + Drug}} X 100

This parameter is crucial for evaluating the efficiency of the production process and minimizing formulation losses.

Selection of optimized batch

On the basis of entrapment efficiency and drug flux and percentage yield the batch with lowest residual value that was close to zero was selected.

Determination of Particle Size and Polydispersity Index

The particle size and polydispersity index (PDI) of optimized batch of FEN-NLC was measured by dynamic light scattering (DLS) at 25°C using a computerized system (Beckman zeta sizer Delsa Nano C, Switzerland, ver. 3.73/2.30. The PDI was determined to find the size distribution of the prepared NLCs. [20]. The measurement was taken at 25° C using disposable sizing cuvette at count rate of 165.6 kcps. Dispersant used was double distilled water having refractive index and viscosity of 1.330 and 0.8800 cP, respectively. The measurement was taken in triplicate (n = 3) after diluting the sample (500×) in dispersant.

Zeta Potential (ζ) Analysis

The optimized batch of FEB-NLC was characterized by zeta potential (**ζ**) analysis using using Beckman Zeta sizer, at 25°C. The measurement was taken using clear disposable zeta cell at count rate of 29.3 kcps. Dispersant used was double distilled water. Measurement was carried out after dilution of sample with dispersant to reach a suitable concentration.

In-vitro release studies

Percentage *in vitro* drug release of the prepared NLC's was determined using dialysis sac method. NLC equivalent to 5mg of Febuxostat were enclosed into the sac tied from both end with a thread. The sac was attached with the shaft of USP type II apparatus and ensured that it remain submerged in 200 ml of phosphate buffer pH 7.4. The temperature was maintained at 37 C and rpm was set at 50. At regular time interval 5 ml sample was removed and analysed spectrophotmetrically at 317 nm [21].

High Resolution Transmission Electron Microscope

Transmission electron microscopy (TEM) images were captured utilizing a JEM 2100 PLUS JEOL device. The preparation of samples involved the dropping of 10 µl of NLCs onto a copper grid containing 10 % phosphotungstic acid [22]. The determination of size distribution was accomplished through the utilization of software to analyze a comprehensive HRTEM image.

Formulation of NLC gel of optimized batch

The weighed quantity of HPMC was mixed in distilled water further addition of triethanolamine to form the hydrogel and also to maintain the desired pH range of the solution (Table). The uniformity was maintained while stirring and further FEB-NLC was incorporated into HPMC gel to obtain nano-gel.

Table 3: Composition of FEB-NLCs loaded topical gel

Ingredients	Quantity taken
FEB-NLCs	6.7% w/w (Eq. 5% w/w FEB)
HPMC	2 % w/w
Triethanolamine	0.30%
Water	q. s

Evaluation of FEB-NLC gel

Determination of the physical appearance

The FEB-NLCs gel was physically examined to determine its color homogeneity, texture consistency, and texture uniformity. The homogeneity of the gel as well as the texture of the gel were both examined by rubbing a little amount of the gel between the index finger and the thumb [23]. The consistency of the gel, as well as the presence or absence of gritty, undissolved components, were taken into consideration in order to determine whether or not the gel is uniform and smooth.

Drug content

One gram of FEB-NLCs-Gel was combined with phosphate buffer pH 6.8 in a standard volumetric flask. The drug content percentage was evaluated by UV-visible spectrophotometry at a wavelength of 317 nm. The following equation (Eq. 3.15) is used to calculate the drug content.

$$\% \text{ Drug content} = \frac{\text{Actual drug content}}{\text{Total drug amount taken}} \times 100$$

Viscosity

The prepared FEB-NLCs Gel was studied for their rheological behavior at 25±1°C using Brookfield viscometer equipped with spindle number S-64 at different shear rates [24].

pH measurement

FEB-NLCs Gel was dispersed in deionized water, and stirred using a magnetic stirrer at room temperature and the pH was determined using a pH meter [25].

Spreadability

Spreadability refers to the capacity of a gel to easily

spread over a wide surface area when applied to the skin or the area that is affected. The measure of spreadability is denoted by the duration, in seconds, required for two slides to slip from a gel substrate, inserted between the two slides, while subjected to a specific load. The shorter the duration required for the separation of two slides, the higher the level of spreadability. A pair of glass slides with standardized dimensions was taken. The Febuxostat NLCs gel formulation was applied on one of the slides. The second slide was mounted on the gel, effectively creating a sandwich with the gel layer in between the two slides. The area in which the gel was contained covered a distance of 6 cm along the length of the slide. A weight of 25 grams was carefully tied to the upper slide. The duration required for the upper slide to traverse a distance of 6cm while being displaced from the lower slide due to weight was recorded. The experiment was carried out three times with both marketed and the formulated gels and the mean time taken by both gels was calculated by using the equation below [26].

Formula $S = M \times L/T$

Where, S is Spreadability

M is Mass in gm (25gm)

L is Length of the glass (6cm) T is Time in sec.

Thermodynamic stability

To assess the thermodynamic stability of the prepared FEB-NLCs Gel, two tests were carried out. In centrifuge stress test, FEB-NLCs Gel was centrifuged at 6,000 rpm for 30 min and then examined for phase separation. In freeze-thaw cycle stress test, FEB-NLCs Gel was subjected to a total of three complete freeze–thaw cycles, each cycle consisting of 24 h at 45°C followed by 24 h at −5°C [27].

***In vitro* release of NLC gel**

The in vitro drug release studies of drug from febuxostat loaded NLCs gel, plain febuxostat gel and physical mixture gel was conducted by using dialysis membrane Franz diffusion cell. A dialysis membrane was placed between the cellular compartments of a Franz diffusion cell. The receptor medium consisting of phosphate buffer with a pH of 6.8 was filled acceptor compartment, and then stirred by magnetic bar to minimize stagnant layers. The gels Febuxostat gel (FEB-G), Febuxostat loaded NLCs gel (FEB-NLCs-G) and physical mixture gel (PM-G) were applied over dialysis membrane. The samples were taken out at different intervals of time (0, 1, 2, 3, 4, 5, 6, 8, 10, 12 and 24 h) and substituted with the same of fresh medium. The amount of drug in the samples were analysed by UV-visible spectrophotometer at 317 nm after making suitable dilutions. All release studies were conducted in triplicate [28].

Stability studies

Long-term and accelerated stability testing of optimized FEN-NLCs-Gel at 5 ± 2oC, 25±2oC/60±5% RH and 40±2°C/75±5 % RH respectively were carried out in in compliance with ICH Q1A (R2) guidelines.

Optimized FEN-NLCs-Gel was characterized for Change in color, Discoloration, consistency, and viscosity at predetermined time intervals i.e. month 0, and after 1, 3, 6, 9 and 12 months of storage. Furthermore, samples were analysed for change in % drug content after 1, 3, 6, 9 and 12 months of storage [29].

***In vivo* Study**

To evaluate the anti-gout efficacy and safety of the febuxastat loaded NLC gel the wistar male rat 180-250 g was used because of their physiological similarity to human in uric acid metabolism. Before starting the study the approval from Institutional Animal Ethical Committee of School of Pharmaceutical Science RIMT University was obtained under Approval letter with reference number RIMT/IAEC/2025/004. The approved numbers of wistar rats 24 were kept under the standard laboratory conditions and provided free access to both water and food and were housed in a room with a 12-hour light-dark cycle for a minimum of three days to ensure proper acclimatization. The experiment was conducted only on healthy rats those who never used in other experiment earlier. CCSEA guidelines were strictly followed for the conduction of experiment on these animals. The obtained animals were divided into 4 groups having six rats in each group for the proposed study. During the study all animals were administered through topical routes

Table:4 Experimental design of in-vivo anti gout efficacy evaluation.

Group	Treatment	Route
I	Normal Control	No induction, Topical placebo gel
II	Disease Control	MSU-induced+Topical placebo gel
III	Standard	MSU-induced+Marketed febuxostat Formulation
IV	Test (Dose)	MSU-induced+febuxostat NLC gel

***In-vivo* Anti-Gout evaluation study**

Local Inflammation Model using Monosodium Urate Crystal

Monosodium Urate Crystal (MSU) induced model was used to induce the gout in which suspension of MSU crystals of concentration 40 mg/ml was prepared in sterile saline and finally the pH was adjusted to 7. The 0.2 ml of prepared MSU

suspension was administered intra-articularly into the rat ankle joint of the right hind paw, whereas control group receives saline injection only. The measured quantity 0.5 g of gel was applied topically on the inflamed joint twice daily for 7 days

The degree of persistent inflammation was evaluated in all the group by measuring the volume and diameter of ankle or joint circumference and paw edema after the 24 hrs of MSU injection by using Vernier caliper and Pethysmometer respectively.

To evaluate the intensity of inflammatory pain, the differences in weight bearing capacity between the normal control and disease control was measured on the 0,1,3,5 and 7th day after injection using randall selitto apparatus. The weight bearing capacity (g) of each joint was calculated over a 10-second period. Each data point was demonstrated as the difference score (g) over the normal control minus disease control and average for three repetitions was calculated. A significant decrease in the difference score (i.e., more negative) after MSU injection was indicated that the animal model of chronic muscle inflammatory pain will be successfully established. To evaluate intensity of inflammation ankle, paw diameter by Verneir caliper and paw volume by digital Plethysmometer was also be measured on 1, 3, 5, 7th day of experiment was also be evaluated [30-32].

RESULTS AND DISCUSSION

Statistical assessment of % EE (Y1)

The quadratic model was found to be statistically significant for %EE based on the fit summary results. The adjusted R^2 (0.9907) and predicted R^2 (0.9532) values differed by less than 0.2 (Table A), suggesting a good correlation between predicted and actual data. The lack of fit p-value (0.0874) was greater than 0.05 (Table B), indicating the model fits the data well and is not significantly flawed. The quadratic model was therefore selected as the best-fit model to interpret the response variable Y1 (%EE). X_1 (Solid:Liquid lipid ratio) and X_2 (Stirring speed) had antagonistic effects (negative coefficients), decreasing %EE. X_3 (Emulsifier concentration) had a synergistic effect (positive coefficient), increasing %EE. The curvature effects (X_1^2, X_2^2, X_3^2) indicate significant quadratic relationships, especially for X_1^2 ($p < 0.01$).

Statistical Assessment of Flux (Y2)

The statistical assessment of the flux (Y2) of Febuxostat-loaded NLCs was performed using Design-Expert® software based on a Box–Behnken design. The quadratic model was found to be most suitable, as evidenced by a minimal difference between adjusted R^2 (0.9846) and predicted R^2 (0.9271), both values being within the acceptable threshold difference of < 0.2. The model p-value was observed to be 0.0123 ($p < 0.05$), confirming that the selected model was statistically significant. The lack of fit p-value was 0.0652 ($p > 0.05$), indicating that the lack of fit was insignificant and the model adequately described the experimental data.

All three independent variables—solid lipid: liquid lipid ratio (X1), stirring speed (X2), and emulsifier concentration (X3)—exhibited significant influence on the flux of Febuxostat ($p < 0.05$). Additionally, the quadratic effects of $X1^2$ and $X3^2$ were also found to be significant ($p < 0.05$), From the regression analysis, the following polynomial equation was obtained for predicting flux (Y2).

Statistical Assessment of % Yield (Y3)

The difference between adjusted R^2 (0.9960) and predicted R^2 (0.9903), as observed from the fit summary statistics, was less than 0.2. The model p-value for Y3 was reported as <0.0001, indicating a statistically significant model ($p < 0.05$). The lack of fit p-value for Y3 was 0.6928 ($p > 0.05$), implying the model fit was appropriate with no significant deviation. Hence, a quadratic model was confirmed as the best fit for predicting % yield.

Among the independent variables, solid lipid: liquid lipid ratio (X1), stirring speed (X2), and emulsifier concentration (X3) had statistically significant effects on Y3 ($p < 0.05$). The quadratic terms of $X1^2$, $X2^2$, and $X3^2$ were also significant, indicating curvature effects. The interaction terms X1X2 and X2X3 were not statistically significant ($p > 0.05$).

The polynomial equation derived for Y3 is:

Y3=73.53+16.55X1−1.95X2−1.23X3−0.8925X1X2 −3.62X12+3.48X22+3.96X32Y_3 = 73.53 + 16.55X_1 - 1.95X_2 - 1.23X_3 - 0.8925X_1X_2 - 3.62X_1^2 + 3.48X_2^2 + 3.96X_3^2Y3 =73.53+16.55X1−1.95X2−1.23X3−0.8925X1X2 −3.62X12+3.48X22+3.96X32

This equation suggests:

X1 (solid:liquid lipid) had a synergistic effect on yield (positive coefficient), X2 (stirring speed) and X3 (emulsifier concentration) had antagonistic effects (negative coefficients). Higher solid lipid content likely promoted particle solidification, increasing yield. However, excessive stirring or surfactant could have led to material loss or unstable emulsification, lowering the yield.

$Y_2 = 104.15 + 5.37X_1 + 14.92X_2 + 12.05X_3 - 1.43X_1X_2 + 0.695X_1X_3 + 5.11X_2X_3 - 2.75X_1^2 - 0.7835X_2^2 - 2.73X_3^2$

This equation suggests a synergistic effect of all three factors on flux, with the stirring speed (X2) showing the strongest contribution ($b_2 = +14.92$), followed by emulsifier concentration (X3) and solid lipid: liquid lipid ratio (X1). These positive coefficients imply that increasing any of the three variables enhances the flux of Febuxostat.

The synergistic effect of increased stirring speed may

be attributed to the formation of smaller NLC particles, which enhance permeation by increasing surface area. Similarly, higher emulsifier concentration likely improved wettability and solubilization of Febuxostat in the lipid matrix, facilitating its diffusion across the membrane. On the other hand, curvature effects ($X1^2$ and $X3^2$) suggest that excessively high lipid ratio or emulsifier concentration may negatively impact flux beyond optimal levels due to possible aggregation or increased viscosity.

Optimization

The optimal values of formulation composition and process variables for optimized FEB-NLCs was found 82.8:17.2 of solid lipid: liquid lipid (X1), 2500 rpm of stirring speed (X2) and 2.5 % of emulsifier concentration (X3) having desirability function of 0.874 as analyzed by Design Expert Software. In addition to this, it gives theoretical/predicted values of EE (%) (Y1), Flux (Y2) and Yield % (Y3) corresponding to 72.98%, 136.19 µg/cm2/h and 92.89%, respectively (Fig.1 a & b).

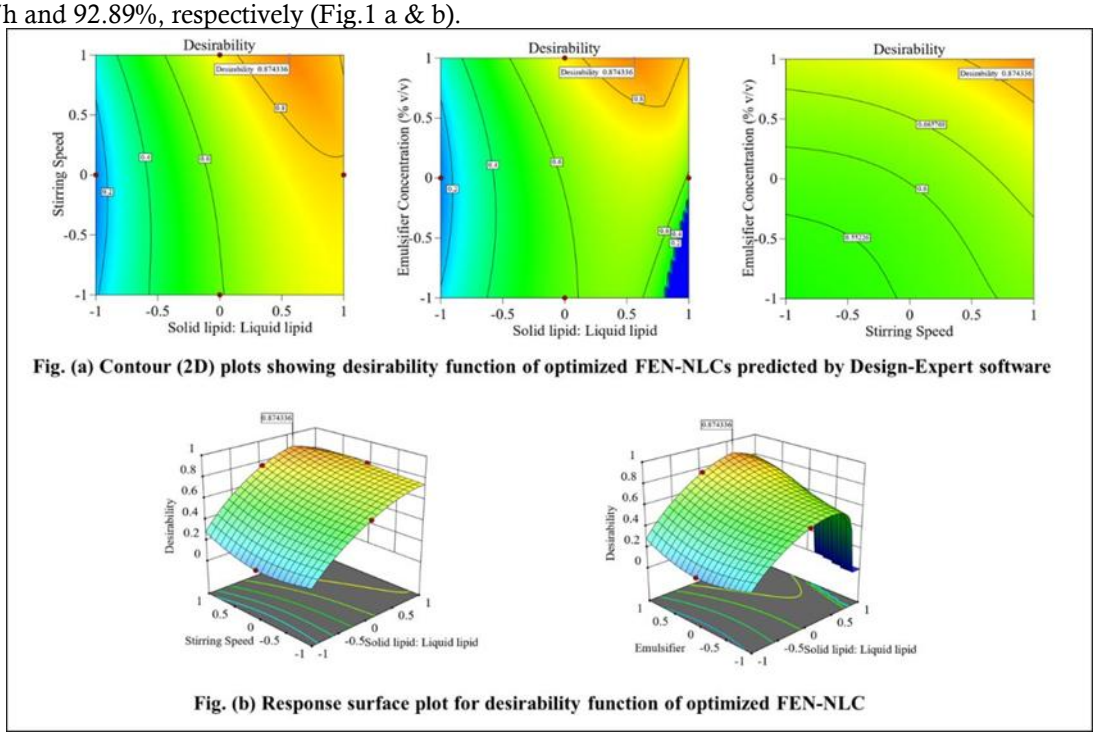

Fig. (a) Contour (2D) plots showing desirability function of optimized FEN-NLCs predicted by Design-Expert software

Fig. (b) Response surface plot for desirability function of optimized FEN-NLC

Figure 1(a): Contour plots and Figure 1(b): 3D surface response showing desirability function of optimized FEB-NLCs.

Particle size and zeta potential

The developed FEB-NLCs showed an average particle size of 344 nm and PDI of 0.309 as depicted in Fig.2. Usually a zeta potential of $\geq \pm 25$ mV is recommended for achieving stable dispersions. The zeta potential was found to be -22.67 mV as shown in Fig. 3. Lower PDI and high negative value of zeta potential suggested homogenous distribution of NLCs and physically stable system without aggregates. This may be achieved due to tween 80 attributed stabilized nanoparticles and negative charge distribution over the surface responsible for repulsion among them. Small size offers a greater surface area for association and permeation through the skin to the deeper layers of tissues.

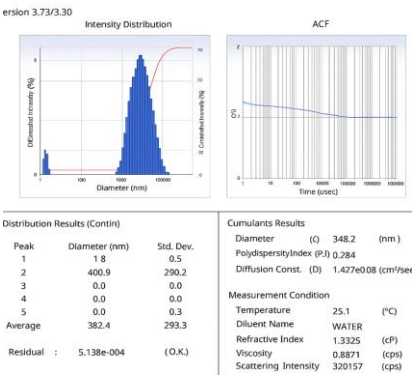

Fig. 2. Particle size of NLCs of Febuxostat

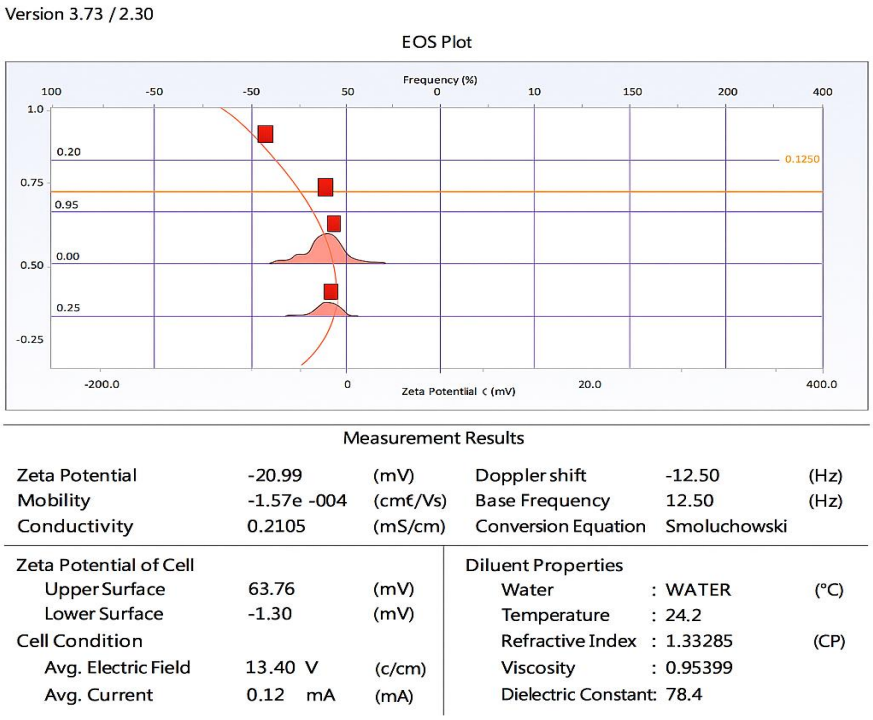

Measurement Results

Zeta Potential	-20.99	(mV)	Doppler shift	-12.50	(Hz)
Mobility	-1.57e -004	(cm€/Vs)	Base Frequency	12.50	(Hz)
Conductivity	0.2105	(mS/cm)	Conversion Equation	Smoluchowski	

Zeta Potential of Cell			Diluent Properties		
Upper Surface	63.76	(mV)	Water	: WATER	(°C)
Lower Surface	-1.30	(mV)	Temperature	: 24.2	
Cell Condition			Refractive Index	: 1.33285	(CP)
Avg. Electric Field	13.40 V	(c/cm)	Viscosity	: 0.95399	
Avg. Current	0.12 mA	(mA)	Dielectric Constant	: 78.4	

Fig. 3 Zeta potential of NLCs of Febuxostat

High Resolution Transmission Electron Microscope (HRTEM) of the FEB- NLCs

The high magnification power of the transmission electron microscope made possible a visual inspection of the spherical nanostructures present in the formulation sample. Fig. 4 depicts NLCs exhibiting a characteristic spherical morphology, with a particle size of 200 nm.

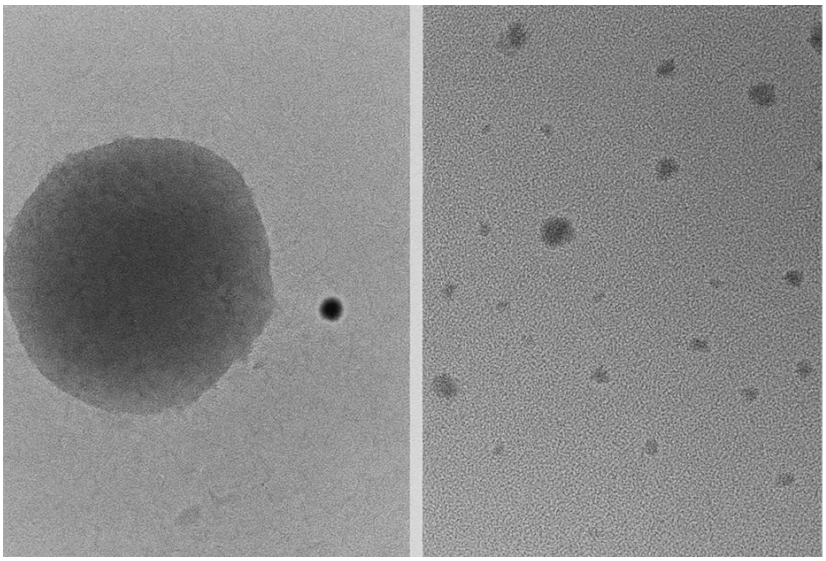

Fig. 4. HRTEM of NLCs of Febuxostat

***In-vitro* release**

The cumulative drug release profile of the prepared formulations was evaluated over a period of 12 hours, as depicted in **Fig. 5**. During the initial phase (first two hours), the nanostructured lipid carrier (NLC) system exhibited a distinct burst release pattern. This rapid release may be attributed to the diffusion of Febuxostat located near or on the surface of the nanoparticles. The optimized batch demonstrated a markedly higher percentage of

drug release compared to the plain drug suspension, which can be ascribed to the increased proportion of liquid lipid in the formulation. The liquid lipid component, predominantly situated in the outer regions of the NLC matrix, enhances the solubilization of hydrophobic drugs and facilitates an initial rapid release phase.
Subsequently, a sustained release pattern was observed, indicating gradual diffusion of the entrapped drug from the solid–lipid matrix into the surrounding medium. The release data were analyzed using various kinetic models—zero-order, first-order, and Higuchi models—to elucidate the mechanism of drug release, as illustrated in **Figure 6**. Among these, the Higuchi model provided the best fit, as reflected by the highest correlation coefficient (R^2) values summarized in **Table 4**. This suggests that the release of Febuxostat from the NLC formulation primarily follows a diffusion-controlled mechanism governed by the drug's movement through the lipid matrix.

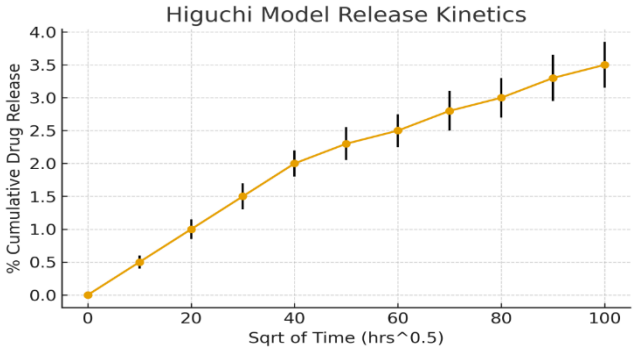

Fig: 5 Higuchi model for obtained drug release

Table 5: R square value and slope of drug release kinetics by different models.

Sr No	Model	R2	Slope
1	Zero Order	0.965	6.381
2	First Order	0.953	-0.054
3	Higuchi equation	0.981	0.039
4	Korsenmeyer Peppas	0.648	1.075

Measurement of Paw volume

Administration of MSU crystal in ankle of right hind paw significantly induced the inflammation and hence the related volume of the same as compared to the normal control. On 7th day it was concluded that treatment with febuxostat NLC gel decrease the paw volume as compare to disease control.

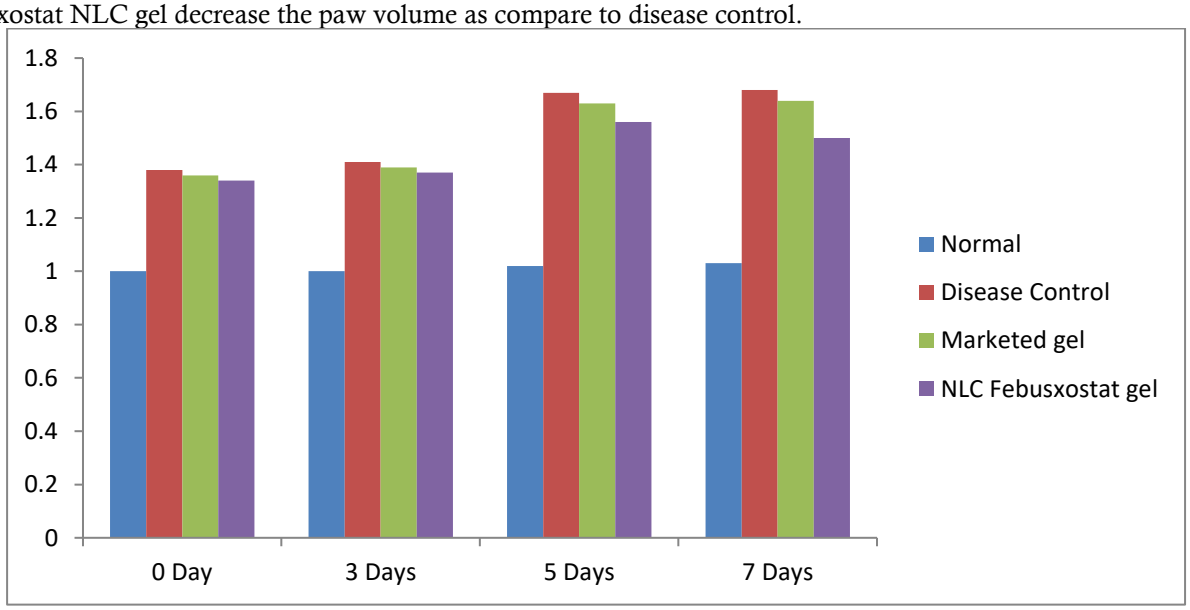

Fig 6: Effect of Febusxostat on change of paw-volume due to inflammation caused by MSU crystal.

Measurement of the ankle circumference/diameter

After injecting MSU crystal in rat ankle to induce gout like condition the ankle got the inflammation and circumference/diameter increased as compare to normal control rats. Similar to the paw volume the

diameter/circumference of the Febuxostat administered rats were found to be significantly reduced

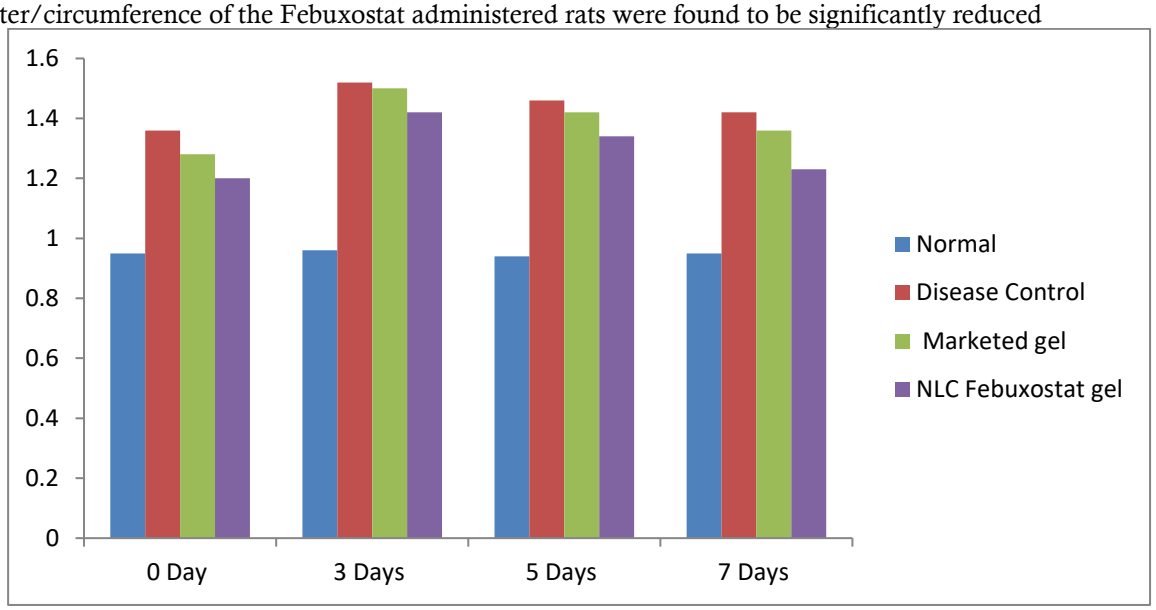

Fig 7: Effect of Febuxostat NLC gel on change in paw diameter in MSU induced inflammation.

Measurement of pain threshold

Randall-Selitto test

At the end of the treatment it was observed NLC gel of Febuxostat increased the pain threshold in the experimental rats as compared to disease control. It was clearly reflected in the conducted experiment that the treated animal got relief in pain and related inflammation.

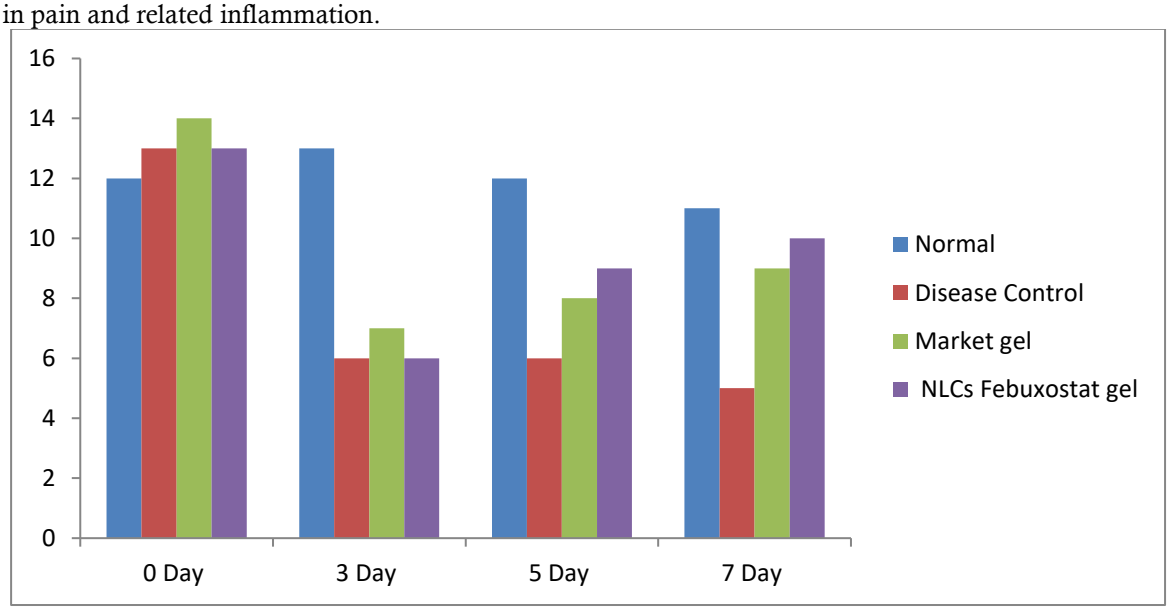

Fig 8: Effect of Febuxostat on change of in pain threshold in MSU crystal induced inflammation.

CONCLUSION

The present study successfully employed a Box–Behnken design to optimize Febuxostat-loaded nanostructured lipid carriers (FEB-NLCs) by systematically evaluating the influence of formulation and process variables on encapsulation efficiency (%EE), transdermal flux, and percentage yield. The quadratic models developed for all three responses (Y_1, Y_2, and Y_3) were found to be statistically significant, as confirmed by high adjusted and predicted R^2 values with differences below 0.2 and insignificant lack-of-fit values ($p > 0.05$). These findings validate the robustness, predictability, and suitability of the selected models for response interpretation and optimization. Encapsulation efficiency was primarily influenced by emulsifier concentration, which exhibited a synergistic effect, while solid-to-liquid lipid ratio and stirring speed showed antagonistic effects. The significant quadratic terms highlighted the presence of curvature effects, emphasizing the importance of maintaining optimal levels of formulation variables. Similarly, flux was significantly affected by all three independent variables, with stirring speed exerting the most pronounced positive effect, followed by emulsifier concentration and lipid ratio. The observed

enhancement in flux can be attributed to reduced particle size, improved wettability, and increased drug solubilization within the lipid matrix. Percentage yield was mainly governed by the solid-to-liquid lipid ratio, which showed a synergistic effect, whereas excessive stirring speed and emulsifier concentration negatively affected yield, likely due to formulation losses or instability at higher levels. Numerical optimization identified the optimal formulation conditions as a solid lipid:liquid lipid ratio of 82.8:17.2, stirring speed of 2500 rpm, and emulsifier concentration of 2.5%, achieving a high desirability value (0.874). Under these conditions, the predicted responses for %EE, flux, and %yield were 72.98%, 136.19 μg/cm²/h, and 92.89%, respectively, demonstrating a favorable balance between drug loading, permeation performance, and production efficiency. The optimized FEB-NLCs exhibited a nanosized particle distribution with a mean particle size of 344 nm, low PDI (0.309), and a moderately high negative zeta potential (−22.67 mV), indicating a homogeneous and physically stable dispersion. HRTEM analysis further confirmed the spherical morphology and nanoscale size of the carriers. In-vitro release studies revealed an initial burst release followed by a sustained release pattern, with drug release best described by the Higuchi model, indicating diffusion-controlled release from the lipid matrix. In-vivo evaluation in an MSU crystal-induced gout model demonstrated significant anti-inflammatory and analgesic efficacy of the Febuxostat NLC gel, as evidenced by reduced paw volume and ankle circumference along with an increased pain threshold compared to disease control animals. These outcomes confirm the improved therapeutic performance of the NLC-based topical delivery system.

Overall, the optimized FEB-NLC formulation demonstrated excellent physicochemical characteristics, controlled drug release, enhanced transdermal flux, and superior in-vivo anti-gout activity. The findings strongly support the potential of Febuxostat-loaded nanostructured lipid carriers as an effective and promising topical delivery system for the management of gout and associated inflammation.

Conflict of Interest All authors of this research declare no conflict of interest.

REFERENCES

1. Perez-Ruiz, Fernando, Nicola Dalbeth, and Tomas Bardin. "A review of uric acid, crystal deposition disease, and gout." Advances in therapy 32, no. 1 (2015): 31-41.
2. Cicero, Arrigo FG, Federica Fogacci, Raffaele Ivan Cincione, Giuliano Tocci, and Claudio Borghi. "Clinical effects of xanthine oxidase inhibitors in hyperuricemic patients." Medical principles and practice 30, no. 2 (2021): 122-130.
3. Jordan, Andreas, and Ursula Gresser. "Side effects and interactions of the xanthine oxidase inhibitor febuxostat." Pharmaceuticals 11, no. 2 (2018): 51.
4. Lin, Zhijian, Jeetendra Kumar Gupta, Mohsin Maqbool, Krishan Kumar, Ayushi Sharma, and Nitin Wahi. "The therapeutic management of chemical and herbal medications on uric acid levels and gout: modern and traditional wisdom." Pharmaceuticals 17, no. 11 (2024): 1507.
5. Kesharwani, Roohi, Pankaj Jaiswal, Dilip Kumar Patel, and Pankaj Kumar Yadav. "Lipid-based drug delivery system (LBDDS): An emerging paradigm to enhance oral bioavailability of poorly soluble drugs." Biomedical Materials & Devices 1, no. 2 (2023): 648-663.
6. Teixeira, M. C., C. Carbone, and E. B. Souto. "Beyond liposomes: Recent advances on lipid based nanostructures for poorly soluble/poorly permeable drug delivery." Progress in lipid research 68 (2017): 1-11.
7. Viegas, Cláudia, Ana B. Patrício, João M. Prata, Akhtar Nadhman, Pavan Kumar Chintamaneni, and Pedro Fonte. "Solid lipid nanoparticles vs. nanostructured lipid carriers: a comparative review." Pharmaceutics 15, no. 6 (2023): 1593.
8. Sivadasan, Durgaramani, Muhammad Hadi Sultan, Osama Madkhali, Yosif Almoshari, and Neelaveni Thangavel. "Polymeric lipid hybrid nanoparticles (plns) as emerging drug delivery platform—A comprehensive review of their properties, preparation methods, and therapeutic applications." Pharmaceutics 13, no. 8 (2021): 1291.
9. Anwer, Md Khalid, Essam A. Ali, Muzaffar Iqbal, Mohammed Muqtader Ahmed, Mohammed F. Aldawsari, Ahmed Al Saqr, Mohd Nazam Ansari, and M. Ali Aboudzadeh. "Development of sustained release baricitinib loaded lipid-polymer hybrid nanoparticles with improved oral bioavailability." Molecules 27, no. 1 (2021): 168.
10. Rangaraj, Nagarjun, Saurabh Shah, Maruthi AJ, Sravanthi Reddy Pailla, Hanumanth Srikanth Cheruvu, and Sunitha Sampathi. "Quality by design approach for the development of self-emulsifying systems for oral delivery of febuxostat: pharmacokinetic and pharmacodynamic evaluation." AAPS PharmSciTech 20, no. 7 (2019): 267.
11. Qazafi, Shehram, Danish Mazhar, Dur E. Nayab, Hussain Ali, Salman Khan, and Saeed Ahmad Khan. "Nanocarrier-Based Approach: Solid Lipid Nanoparticles for the Enhanced Bioavailability of Febuxostat." BioNanoScience 15, no. 2 (2025): 1-18.
12. Alshahrani, Saad M., Hadil Faris Alotaibi, and Mohammed Alqarni. "Modeling and validation

of drug release kinetics using hybrid method for prediction of drug efficiency and novel formulations." Frontiers in Chemistry 12 (2024): 1395359.
13. Qazafi, Shehram, Danish Mazhar, Dur E. Nayab, Hussain Ali, Salman Khan, and Saeed Ahmad Khan. "Nanocarrier-Based Approach: Solid Lipid Nanoparticles for the Enhanced Bioavailability of Febuxostat." BioNanoScience 15, no. 2 (2025): 1-18.
14. Maddukuri, Muralikrishna. "Formulation and Evaluation of Solid Lipid Microparticles of Clopidogrel." Master's thesis, Rajiv Gandhi University of Health Sciences (India), 2013.
15. Ramadan, Alyaa Adel. "A study of some lipid-based drug delivery systems." PhD diss., Université d'Angers, 2010.
16. Gurumukhi, Vishal C., Vivek P. Sonawane, Ganesh G. Tapadiya, Sanjaykumar B. Bari, Sanjay J. Surana, and Shailesh S. Chalikwar. "Quality-by-design based fabrication of febuxostat-loaded nanoemulsion: statistical optimization, characterizations, permeability, and bioavailability studies." Heliyon 9, no. 4 (2023).
17. Radwan, Ibrahim Taha, Mohamed Z. Sayed-Ahmed, Nirvina AbdelRaouf Ghazawy, Saad S. Alqahtani, Sarfaraz Ahmad, Nawazish Alam, Abeer Mousa Alkhaibari, Md Sajid Ali, Abdelfattah Selim, and Eman Alaaeldin AbdelFattah. "Effect of nanostructure lipid carrier of methylene blue and monoterpenes as enzymes inhibitor for Culex pipiens." Scientific Reports 13, no. 1 (2023): 12522.
18. Müller, Rainer H., Monika Radtke, and Sabine A. Wissing. "Solid Lipid Nanoparticles (SLN) and Nanostructured Lipid Carriers (NLC) in Cosmetic and Dermatological Preparations." Advanced Drug Delivery Reviews 54, no. 1 (2002): S131–S155.
19. Mehnert, Wolfgang, and Karsten Mäder. "Solid Lipid Nanoparticles: Production, Characterization and Applications." Advanced Drug Delivery Reviews 47, no. 2–3 (2001): 165–196.
20. Malvern Instruments, "Dynamic Light Scattering (DLS): An Introduction in 30 Minutes." Malvern Technical Note, United Kingdom (2012): 1–20.
21. Higuchi, Takeru. "Mechanism of Sustained-Action Medication: Theoretical Analysis of Rate of Release of Solid Drugs Dispersed in Solid Matrices." Journal of Pharmaceutical Sciences 52, no. 12 (1963): 1145–1149.
22. Bozzuto, Giuseppina, and Anna Molinari. "Liposomes as Nanomedical Devices."
23. International Journal of Nanomedicine 10 (2015): 975–999.
24. Gupta, G. D., and R. S. Gaud. "Development and Evaluation of Niosomal Gel Formulation for Topical Application." Asian Journal of Pharmaceutical Sciences 2, no. 3 (2007): 94–100.
25. Sinko, Patrick J. "Rheological Properties and Evaluation of Semisolid Dosage Forms." In Martin's Physical Pharmacy and Pharmaceutical Sciences, 6th ed. Philadelphia: Lippincott Williams & Wilkins (2011): 635–650.
26. Lachman, Leon, Herbert A. Lieberman, and Joseph L. Kanig. "Theory and Practice of Semisolid Dosage Forms." In The Theory and Practice of Industrial Pharmacy, 3rd ed. Philadelphia: Lea & Febiger (1986): 534–563.
27. Mutalik, Srinivas, and D. Hiremath. "Effect of Chitosan on the Properties of Transdermal Films of Ketorolac Tromethamine." Indian Journal of Pharmaceutical Sciences 64, no. 5 (2002): 469–473.
28. Shakeel, Faiyaz, Sanjula Baboota, Alka Ahuja, Javed Ali, and Shadab Shafiq.
29. "Stability Evaluation of Celecoxib Nanoemulsion Containing Tween 80."
30. AAPS PharmSciTech 9, no. 1 (2008): 53–59.
31. Kakkar, Varun, Sreekanth Kumar Muppu, Kanwaljit Chopra, and Indu Pal Kaur.
32. "Formulation and Evaluation of Lecithin-Based Nanostructured Lipid Carriers of Curcumin for Topical Application." Journal of Microencapsulation 27, no. 6 (2010): 507–522.
33. International Council for Harmonisation (ICH). "ICH Q1A (R2): Stability Testing of New Drug Substances and Products." ICH Harmonised Guideline, Geneva (2003): 1–24.
34. Coderre, Terence J., and Patrick D. Wall. "Ankle Joint Urate Arthritis in Rats Provides a Useful Tool for the Evaluation of Analgesic and Anti-Inflammatory Agents." Pain 34, no. 2 (1988): 143–152.
35. Schlesinger, Naomi." Monosodium Urate Crystal-Induced Inflammation: Pathogenesis and Treatment of Gout." Rheumatic Disease Clinics of North America 40, no. 2 (2014): 235–247.
36. Hsieh, Shu-Chen, Tzu-Yu Tsai, Yi-Jen Lin, and Chung-Hung Chen. "Topical Anti-Inflammatory Effects of Herbal Formulations in Monosodium Urate-Induced Gouty Arthritis in Rats." Journal of Ethnopharmacology 134, no. 2 (2011): 466–472.

